

## Deconfined Quantum Critical Points

T. Senthil,<sup>1\*</sup> Ashvin Vishwanath,<sup>1</sup> Leon Balents,<sup>2</sup> Subir Sachdev,<sup>3</sup> Matthew P. A. Fisher<sup>4</sup>

The theory of second-order phase transitions is one of the foundations of modern statistical mechanics and condensed-matter theory. A central concept is the observable order parameter, whose nonzero average value characterizes one or more phases. At large distances and long times, fluctuations of the order parameter(s) are described by a continuum field theory, and these dominate the physics near such phase transitions. We show that near second-order quantum phase transitions, subtle quantum interference effects can invalidate this paradigm, and we present a theory of quantum critical points in a variety of experimentally relevant two-dimensional antiferromagnets. The critical points separate phases characterized by conventional “confining” order parameters. Nevertheless, the critical theory contains an emergent gauge field and “deconfined” degrees of freedom associated with fractionalization of the order parameters. We propose that this paradigm for quantum criticality may be the key to resolving a number of experimental puzzles in correlated electron systems and offer a new perspective on the properties of complex materials.

Much recent research in condensed-matter physics has focused on the behavior of matter near zero-temperature “quantum” phase transitions that are seen in several strongly correlated many-particle systems (1). Indeed, a popular view ascribes many properties of correlated materials to the competition between qualitatively distinct ground states and the associated phase transitions. Examples of such materials include the cuprate high-temperature superconductors and the rare earth intermetallic compounds (known as the heavy fermion materials).

The traditional guiding principle behind the modern theory of critical phenomena is the association of the critical singularities with fluctuations of an order parameter that encapsulates the difference between the two phases on either side of the critical point (a simple example is the average magnetic moment, which distinguishes ferromagnetic iron at room temperature from its high-temperature paramagnetic state). This idea, developed by Landau and Ginzburg (2), has been eminently successful in describing a wide variety of phase-transition phenomena. It culminated in the

sophisticated renormalization group theory of Wilson (3), which gave a general prescription for understanding the critical singularities. Such an approach has been adapted to examine quantum critical phenomena as well and provides the generally accepted framework for theoretical descriptions of quantum transitions.

We present specific examples of quantum phase transitions that do not fit into this Landau-Ginzburg-Wilson (LGW) paradigm (4). The natural field theoretic description of their critical singularities is not in terms of the order parameter field(s) that describe the bulk phases, but in terms of new degrees of freedom specific to the critical point. In our examples, there is an emergent gauge field that mediates interactions between emergent particles that carry fractions of the quantum numbers of the underlying degrees of freedom. These fractional particles are not present (that is, are confined) at low energies on either side of the transition but appear naturally at the transition point. Laughlin has previously argued for fractionalization at quantum critical points on phenomenological grounds (5).

We present our examples using phase transitions in two-dimensional (2D) quantum magnetism, although other points of view are also possible (6). Consider a system of spin  $S = 1/2$  moments  $\vec{S}_r$  on the sites,  $r$ , of a 2D square lattice with the Hamiltonian

$$H = J \sum_{\langle rr' \rangle} \vec{S}_r \cdot \vec{S}_{r'} + \dots \quad (1)$$

where  $J > 0$  is the antiferromagnetic ex-

change interaction, and the ellipses represent other short-range interactions that may be tuned to drive various zero-temperature phase transitions.

Considerable progress has been made in elucidating the possible ground states of such a Hamiltonian. The Néel state has long-range magnetic order (Fig. 1A) and has been observed in a variety of insulators, including the prominent parent compound of the cuprates:  $\text{La}_2\text{CuO}_4$ . Apart from such magnetic states, it is now recognized that models in the class of  $H$  can exhibit a variety of quantum paramagnetic ground states. In such states, quantum fluctuations prevent the spins from developing magnetic long-range order. One class of paramagnetic states is the valence bond solids (VBS) (Fig. 1B). In such states, pairs of nearby spins form a singlet, resulting in an ordered pattern of valence bonds. Typically, such VBS states have an energy gap to spin-carrying excitations. Furthermore, for spin-1/2 systems on a square lattice, such states also necessarily break lattice translational symmetry. A second class of paramagnets has a liquid of valence bonds and need not break lattice translational symmetry, but we will not consider such states here. Our focus is on the nature of the phase transition between the ordered magnet and a VBS. We also restrict our discussion to the simplest kinds of ordered antiferromagnets: those with collinear order, where the order parameter is a single vector (the Néel vector).

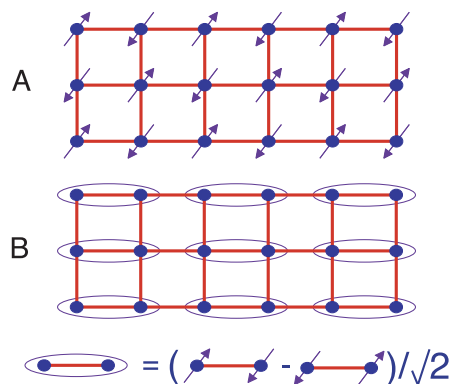


**Fig. 1.** (A) The magnetic Néel ground state of the Hamiltonian Eq. 1 on the square lattice. The spins,  $\vec{S}_r$ , fluctuate quantum-mechanically in the ground state, but they have a nonzero average magnetic moment, which is oriented along the directions shown. (B) A VBS quantum paramagnet. The spins are paired in singlet valence bonds, which resonate among the many different ways the spins can be paired up. The valence bonds crystallize, so that the pattern of bonds shown has a larger weight in the ground state wavefunction than its symmetry-related partners (obtained by 90° rotations of the above states about a site). This ground state is therefore fourfold degenerate.

<sup>1</sup>Department of Physics, Massachusetts Institute of Technology, Cambridge, MA 02139, USA. <sup>2</sup>Department of Physics, University of California, Santa Barbara, CA 93106–4030, USA. <sup>3</sup>Department of Physics, Yale University, P.O. Box 208120, New Haven, CT 06520–8120, USA. <sup>4</sup>Kavli Institute for Theoretical Physics, University of California, Santa Barbara, CA 93106–4030, USA.

\*To whom correspondence should be addressed. E-mail: senthil@mit.edu

Both the magnetic Néel state and the VBS are states of broken symmetry. The former breaks spin rotation symmetry and the latter that of lattice translations. The order parameters associated with these two different broken symmetries are very different. A LGW description of the competition between these two kinds of orders generically predicts either a first-order transition or an intermediate region of coexistence where both orders are simultaneously present. A direct second-order transition between these two broken symmetry phases requires fine-tuning to a multicritical point. Our central thesis is that for a variety of physically relevant quantum systems, such canonical predictions of LGW theory are incorrect. For  $H$ , we will show that a generic second-order transition is possible between the very different kinds of broken symmetry in the Néel and VBS phases. Our critical theory for this transition is, however, unusual and is not naturally described in terms of the order parameter fields of either phase. A picture related to the one developed here applies also to transitions between valence bond liquid and VBS states (7) and to transitions between different VBS states (8) in the quantum dimer model (9, 10).

**Field theory and topology of quantum antiferromagnets.** In the Néel phase or close to it, the fluctuations of the Néel order parameter are captured correctly by the well-known  $O(3)$  nonlinear sigma model field theory (11–13), with the following action  $S_n$  in spacetime [we have promoted the lattice coordinate  $r = (x, y)$  to a continuum spatial coordinate, and  $\tau$  is imaginary time]:

$$S_n = \frac{1}{2g} \int d\tau \int d^2r \left[ \frac{1}{c^2} \left( \frac{\partial \hat{n}}{\partial \tau} \right)^2 + (\nabla_r \hat{n})^2 \right] + iS \sum_r (-1)^r A_r \quad (2)$$

Here  $\hat{n} \propto (-1)^r \vec{S}_r$  is a unit three-component vector that represents the Néel order parameter [the factor  $(-1)^r$  is +1 on one checkerboard sublattice and -1 on the other]. The second term is the quantum-mechanical Berry phase of all the  $S = 1/2$  spins:  $A_r$  is the area enclosed by the path mapped by the time

evolution of  $\hat{n}_r$  on a unit sphere in spin space. These Berry phases play an unimportant role in the low-energy properties of the Néel phase (12) but are crucial in correctly describing the quantum paramagnetic phase (14). We show here that they also modify the quantum critical point between these phases, so that the exponents are distinct from those of the LGW theory without the Berry phases studied earlier (12, 15).

To describe the Berry phases, first note that in two spatial dimensions, smooth configurations of the Néel vector admit topological textures known as skyrmions (Fig. 2). The total skyrmion number associated with a configuration defines an integer topological quantum number  $Q$

$$Q = \frac{1}{4\pi} \int d^2r \hat{n} \cdot \partial_x \hat{n} \times \partial_y \hat{n} \quad (3)$$

The sum over  $r$  in Eq. 2 vanishes (1, 11) for all spin time histories with smooth equal-time configurations, even if they contain skyrmions. For such smooth configurations, the total skyrmion number  $Q$  is independent of time. However, the original microscopic model is defined on a lattice, and processes where  $Q$  changes by some integer amount are allowed. Specifically, such a  $Q$  changing event corresponds to a monopole (or hedgehog) singularity of the Néel field  $\hat{n}(r, \tau)$  in spacetime (a hedgehog has  $\hat{n}$  oriented radially outward in all spacetime directions away from its center). Haldane (11) showed that the sum over  $r$  in Eq. 2 is nonvanishing in the presence of such monopole events. Precise calculation (11) gives a total Berry phase associated with each such  $Q$  changing process, which oscillates rapidly on four sublattices of the dual lattice. This leads to destructive interference, which effectively suppresses all monopole events unless they are quadrupled (11, 14) (that is, they change  $Q$  by 4).

The sigma model field theory augmented by these Berry phase terms is, in principle, powerful enough to correctly describe the quantum paramagnet. Summing over the various monopole tunneling events shows that in the paramagnetic phase, the presence of the

Berry phases leads to VBS order (14). Thus,  $S_n$  contains within it the ingredients describing both the ordered phases of  $H$ . However, a description of the transition between these phases has so far proved elusive and will be provided here.

Our analysis of this critical point is aided by writing the Néel field  $\hat{n}$  in the so-called  $CP^1$  parametrization

$$\hat{n} = z^\dagger \vec{\sigma} z \quad (4)$$

with  $\vec{\sigma}$  a vector of Pauli matrices. Here  $z = z(r, \tau) = (z_1, z_2)$  is a two-component complex spinor of unit magnitude, which transforms under the spin-1/2 representation of the  $SU(2)$  group of spin rotations. The  $z_{1,2}$  are the fractionalized “spinon” fields. To understand the monopoles in this representation, let us recall that the  $CP^1$  representation has a  $U(1)$  gauge redundancy. Specifically, the local phase rotation

$$z \rightarrow e^{i\gamma(r, \tau)} z \quad (5)$$

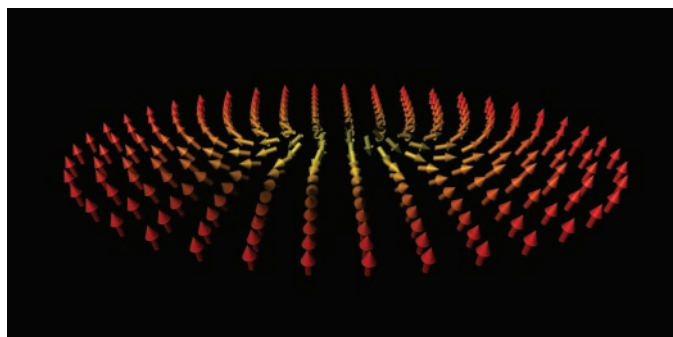
leaves  $\hat{n}$  invariant and hence is a gauge of degree of freedom. Thus, the spinon fields are coupled to a  $U(1)$  gauge field,  $a_\mu$  [the space-time index  $\mu = (r, \tau)$ ]. As is well known, the magnetic flux of  $a_\mu$  is the topological charge density of  $\hat{n}$  appearing in the integrand of Eq. 3. Specifically, configurations where the  $a_\mu$  flux is  $2\pi$  correspond to a full skyrmion (in the ordered Néel phase). Thus, the monopole events described above are spacetime magnetic monopoles (instantons) of  $a_\mu$  at which  $2\pi$  gauge flux can either disappear or be created. The fact that such instanton events are allowed means that the  $a_\mu$  gauge field is to be regarded as compact.

We now state our key result for the critical theory between the Néel and VBS phases. We argue below that the Berry phase-induced quadrupling of monopole events renders monopoles irrelevant at the quantum critical point. So in the critical regime (but not away from it in the paramagnetic phase), we may neglect the compactness of  $a_\mu$  and write down the simplest critical theory of the fractionalized spinons interacting with a noncompact  $U(1)$  gauge field with action  $S_z = \int d^2r d\tau L_z$  and

$$L_z = \sum_{\alpha=1}^N |(\partial_\mu - ia_\mu) z_\alpha|^2 + s|z|^2 + u(|z|^2)^2 + \kappa(\epsilon_{\mu\nu\kappa} \partial_\nu a_\kappa)^2 \quad (6)$$

Where  $N = 2$  is the number of  $z$  components, we have softened the length constraint on the spinons, with  $|z|^2 \equiv \sum_{\alpha=1}^N |z_\alpha|^2$  allowed to fluctuate and the value of  $s$  is to be tuned so that  $L_z$  is at its scale-invariant critical point. The irrelevance of monopole tunneling events at the critical fixed point implies that the total gauge flux  $\int d^2r (\partial_x a_y - \partial_y a_x)$ , or equivalently the skyrmion number  $Q$ , is as-

**Fig. 2.** A skyrmion configuration of the field  $\hat{n}(r)$ . Note that  $\hat{n} = (-1)^r \vec{S}_r$ , and so the underlying spins have a rapid sublattice oscillation, which is not shown. The skyrmion above has  $\hat{n}(r=0) = (0, 0, -1)$  and  $\hat{n}(|r| \rightarrow \infty) = (0, 0, 1)$ .



ymptotically conserved. This emergent global topological conservation law provides precise meaning to the notion of deconfinement. It is important to note that the critical theory described by  $L_z$  (16) is distinct from the LGW critical theory of the O(3) nonlinear sigma model obtained from Eq. 2 by dropping the Berry phases and tuning  $g$  to a critical value (17). In particular, the latter model has a nonzero rate of monopole tunneling events at the transition, so that the global skyrmion number  $Q$  is not conserved.

Among the important physical consequences of the theory  $L_z$  (7, 18) are the presence of two diverging length scales upon approaching the critical point from the VBS side (the spin correlation length and a longer scale beyond which two spinons interact with a linear confining potential) and a large anomalous dimension for the Néel order parameter (because it is a composite of the critical spinons).

The critical theory  $L_z$  is actually implied by existing results in the  $N \rightarrow \infty$  limit (18). The following section illustrates the origin of  $L_z$  by a physical derivation for the case of “easy-plane” anisotropy, when the spins prefer to lie in the  $xy$  plane. Such arguments can be generalized to the isotropic case (7, 18).

**Duality transformations with easy-plane anisotropy.** For the easy-plane case, duality maps and an explicit derivation of a dual form of  $L_z$  are already available in the literature (6, 19). Here we obtain this theory using simple physical arguments.

The easy-plane anisotropy reduces the continuous SU(2) spin rotational invariance to the U(1) subgroup of rotations about the  $z$  axis of spin, along with a  $Z_2$  (Ising) spin reflection symmetry along the  $z$  axis. With these symmetries, Eq. 2 allows an additional term  $u_{ep} \int d\tau d^2r (n^z)^2$ , with  $u_{ep} > 0$ .

The classical Néel ground state of the easy-plane model  $\hat{n}$  is independent of position and lies in the spin  $xy$  plane. Topological defects above this ground state play an important role. These are vortices in the complex field  $n^+ = n_x + in_y$ , and along a large loop around the vortex the phase of  $n^+$  winds by  $2\pi m$ , with  $m$  an integer. In the core, the XY order is suppressed and the  $\hat{n}$  vector will point along the  $\pm\hat{z}$  direction. This corresponds to a nonzero staggered magnetization of the  $z$  component of the spin in the core region. Thus, at the classical level, there are two kinds of vortices, often called merons, depending on the direction of the  $\hat{n}$  vector at the core (Fig. 3). Either kind of vortex breaks the Ising-like  $n^z \rightarrow -n^z$  symmetry at the core. Let us denote by  $\Psi_1$  the quantum field that destroys a vortex whose core points in the up direction and by  $\Psi_2$  the quantum field that destroys a vortex whose core points in the down direction.

Clearly, this breaking of the Ising symmetry is an artifact of the classical limit: Once

quantum effects are included, the two broken symmetry cores will be able to tunnel into each other, and there will be no true broken Ising symmetry in the core. This tunneling is often called an “instanton” process that connects two classically degenerate states.

Surprisingly, such an instanton event is physically the easy-plane avatar of the spacetime monopole described above for the fully isotropic model. This may be seen pictorially. Each classical vortex of Fig. 3 really represents half of the skyrmion configuration of Fig. 2. Now imagine the  $\Psi_2$  meron at time  $\tau \rightarrow -\infty$  and the  $\Psi_1$  meron at time  $\tau \rightarrow \infty$ . These two configurations cannot be smoothly connected, and there must be a singularity in the  $\hat{n}$  configuration, which we place at the origin of spacetime. A glance at Fig. 3 shows that the resulting configuration of  $\hat{n}$  can be smoothly distorted into the radially symmetric hedgehog/monopole event. Thus, the tunneling process between the two merons is equivalent to creating a full skyrmion. This is precisely the monopole event. Hence, a skyrmion may be regarded as a composite of an “up” meron and a “down” antimeron, and the skyrmion number is the difference in the numbers of up and down merons.

The picture so far has not accounted for the Berry phases. The interference effect discussed above for isotropic antiferromagnets applies here too, leading to an effective cancellation of instanton tunneling events between single  $\Psi_1$  and  $\Psi_2$  merons. The only effective tunnelings are those in which four  $\Psi_1$  merons come together and collectively flip their core spins to produce four  $\Psi_2$  merons, or vice versa.

A different perspective on the  $\Psi_{1,2}$  meron vortices is provided by the CP<sup>1</sup> representation. Ordering in the  $xy$  plane of spin space requires condensing the spinons

$$|\langle z_1 \rangle| = |\langle z_2 \rangle| \neq 0 \quad (7)$$

so that  $n^+ = z_1^* z_2$  is ordered and there is no average value of  $n^z = |z_1|^2 - |z_2|^2$ . Now, clearly, a full  $2\pi$  vortex in  $n^+$  can be achieved by either having a  $2\pi$  vortex in  $z_1$  and not in  $z_2$ , or a  $2\pi$  antivortex in  $z_2$  and no

vorticity in  $z_1$ . In the first choice, the amplitude of the  $z_1$  condensate will be suppressed at the core, but  $\langle z_2 \rangle$  will be unaffected. Consequently,  $n^z = |z_1|^2 - |z_2|^2$  will be nonzero and negative in the core, as in the  $\Psi_2$  meron. The other choice also leads to nonzero  $n^z$ , which will now be positive, as in the  $\Psi_1$  meron. Clearly, we may identify the  $\Psi_2$  ( $\Psi_1$ ) meron vortices with  $2\pi$  vortices (antivortices) in the spin fields  $z_1$  ( $z_2$ ). Note that in terms of the spinons, paramagnetic phases correspond to situations in which neither spinon field is condensed.

The above considerations and the general principles of boson duality in three spacetime dimensions (20) determine the form of the dual action  $S_{\text{dual}} = \int d\tau d^2r L_{\text{dual}}$  for  $\Psi_{1,2}$  (6, 19)

$$\begin{aligned} L_{\text{dual}} = & \sum_{\alpha=1,2} |(\partial_\mu - iA_\mu)\Psi_\alpha|^2 + r_d |\Psi|^2 \\ & + u_d (|\Psi|^2)^2 + v_d |\Psi_1|^2 |\Psi_2|^2 \\ & + \kappa_d (\epsilon_{\mu\nu\kappa} \partial_\nu A_\kappa)^2 - \lambda [(\Psi_2^* \Psi_2)^4 \\ & + (\Psi_2^* \Psi_1)^4] \end{aligned} \quad (8)$$

where

$$|\Psi|^2 = |\Psi_1|^2 + |\Psi_2|^2$$

The correctness of this form may be argued as follows: First, from the usual boson-vortex duality transformation (20), the dual  $\Psi_{1,2}$  vortex fields must be minimally coupled to a dual noncompact U(1) gauge field  $A_\mu$ . This dual gauge invariance is not related to Eq. 5 but is a consequence of the conservation of the total  $S^z$ : the “magnetic” flux  $\epsilon_{\mu\nu\kappa} \partial_\nu A_\kappa$  is the conserved  $S^z$  current (20). Second, under the  $Z_2$  reflection symmetry, the two vortices get interchanged; that is,  $\Psi_1 \leftrightarrow \Psi_2$ . The dual action must therefore be invariant under interchange of the 1 and 2 labels. Finally, if monopole events were to be disallowed by hand, the total skyrmion number - (the difference in the number of up and down meron vortices) would be conserved. This would imply a global U(1) symmetry [not to be confused with the U(1) spin symmetry about

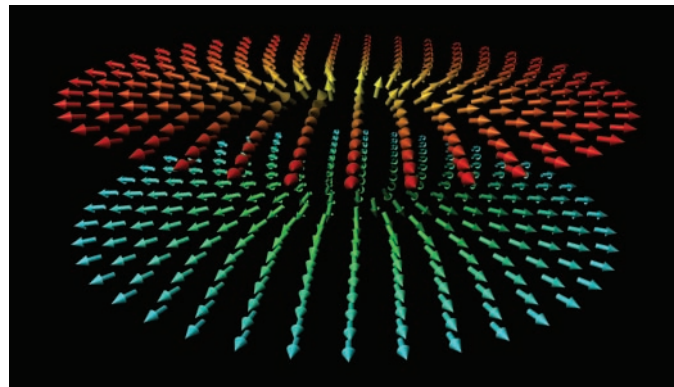


**Fig. 3.** The meron vortices  $\Psi_1$  (above) and  $\Psi_2$  in the easy-plane case. The  $\Psi_1$  meron above has  $\hat{n}$  ( $r=0$ ) = (0,0,1) and  $\hat{n}$  ( $|r| \rightarrow \infty$ ) =  $(xy,0)/|r|$ ; the  $\Psi_2$  meron has  $\hat{n}$  ( $r=0$ ) = (0,0,-1) and the same limit as  $|r| \rightarrow \infty$ . Each meron above is half the skyrmion in Fig. 2: A composite of  $\Psi_1$  and  $\Psi_2^*$  makes one skyrmion.



the  $z$  axis] under which

$$\Psi_1 \rightarrow \Psi_1 \exp(i\phi); \Psi_2 \rightarrow \Psi_2 \exp(-i\phi) \quad (9)$$

where  $\phi$  is a constant. However, monopole events destroy the conservation of skyrmion number and hence this dual global U(1) symmetry. But because the monopoles are effectively quadrupled by cancellations from the Berry phases, skyrmion number is still conserved modulo 4. Thus, the symmetry in Eq. 9 must be broken down to the discrete cyclic group of four elements,  $Z_4$ .

The dual Lagrangian in Eq. 8 is the simplest one that is consistent with all these requirements. In particular, we note that in the absence of the  $\lambda$  term, the dual global U(1) transformation in Eq. 9 leaves the Lagrangian invariant. The  $\lambda$  term breaks this down to  $Z_4$  as required. Thus, we may identify this term with the quadrupled monopole tunneling events. Berry phases are therefore explicitly included in  $L_{\text{dual}}$ .

In this dual vortex theory, the XY ordered phase is simply characterized as a dual “paramagnet,” where  $\langle \Psi_{1,2} \rangle = 0$  and fluctuations of  $\Psi_{1,2}$  are gapped. On the other hand, spin paramagnetic phases such as the VBS states correspond to condensates of the fields  $\Psi_{1,2}$ , which break the dual gauge symmetry. In particular, if both  $\Psi_1$  and  $\Psi_2$  condense with equal amplitude  $|\langle \Psi_1 \rangle| = |\langle \Psi_2 \rangle| \neq 0$ , then we obtain a paramagnetic phase where the global Ising symmetry is preserved. Note the remarkable complementarity between the description of the phases in this dual theory with that in terms of the spinon fields of the  $CP^1$  representation: The descriptions map onto one another upon interchanging both  $z_{1,2} \leftrightarrow \Psi_{1,2}$  and the role of the XY ordered and paramagnetic phases. This is a symptom of an exact duality between the two descriptions that obtains close to the transition (17, 18).

The combination  $\Psi^*_1 \Psi_2 \equiv |\Psi_1 \Psi_2| e^{i(\theta_1 - \theta_2)}$  actually serves as an order parameter for the translation symmetry–broken VBS ground state. This may be seen from the analysis of (6, 19). Alternatively, we may use the identification (14) of the skyrmion creation operator with the order parameter for translation symmetry breaking.

Such a condensate of  $\Psi_{1,2}$  breaks the global  $Z_4$  symmetry of the action in Eq. 8. The preferred direction of the angle  $\theta_1 - \theta_2$  depends on the sign of  $\lambda$ . The two sets of preferred directions correspond to columnar and plaquette patterns of translational symmetry breaking (Fig. 4). Also, the breaking of the dual U(1) symmetry in Eq. 9 by  $\lambda$  corresponds to a linear confinement of spinons in the paramagnet.

Despite its importance in the paramagnet, the  $\lambda$  term is irrelevant at the critical point (18). In critical phenomena parlance, it is a dangerously irrelevant perturbation (15). Consequently the critical theory is deconfined, and the  $z_{1,2}$  spinons (which are fractions of  $n^+$ ), or in the dual description the  $\Psi_{1,2}$  merons (which are fractions of a skyrmion), emerge as natural degrees of freedom right at the critical point. The spinons are confined in both adjacent phases, but the confinement length scale diverges on approaching the critical point. At a more sophisticated level, the critical fixed point is characterized by the emergence of an extra global U(1) symmetry in Eq. 9 that is not present in the microscopic Hamiltonian. This is associated with the conservation of skyrmion number and follows from the irrelevance of monopole tunneling events only at the critical point.

The absence of monopoles at the critical point, when generalized to the isotropic case (18), provides one of the justifications for the claimed critical theory in Eq. 6.

**Discussion.** Our results offer a new perspective on the phases of Mott insulators in two dimensions: Liquid resonating–valence–bond-like states, with gapless spinon excitations, can appear at isolated critical points between phases characterized by conventional confining orders. It appears probable that similar considerations apply to quantum critical points in doped Mott insulators, between phases with a variety of spin- and charge-density-wave orders and  $d$ -wave superconductivity. If so, the electronic properties in the quantum critical region of such critical points will be strongly non-Fermi-liquid-like, raising the prospect of understanding the phenomenology of the cuprate superconductors.

On the theoretical side, our results also

illuminate studies of frustrated quantum antiferromagnets in two dimensions. A theory of the observed critical point between the Néel and VBS phases (21) is now available, and precise tests of the values of critical exponents should now be possible. A variety of other SU(2)-invariant antiferromagnets have been studied (22), and many of them exhibit VBS phases. It would be interesting to explore the characteristics of the quantum critical points adjacent to these phases and test our prediction of deconfinement at such points.

Our results also caricature interesting phenomena (23, 24) in the vicinity of the onset of magnetism in the heavy fermion metals. Remarkably, the Kondo coherence that characterizes the nonmagnetic heavy Fermi liquid seems to disappear at the same point at which magnetic long-range order sets in. Furthermore, strong deviations from Fermi liquid theory are seen in the vicinity of the quantum critical point. All of this is in contrast to naive expectations based on the LGW paradigm for critical phenomena. However, this kind of exotic quantum criticality between two conventional phases is precisely the physics discussed in the present paper.

#### References and Notes

1. S. Sachdev, *Quantum Phase Transitions* (Cambridge Univ. Press, Cambridge, 1999).
2. L. D. Landau, E. M. Lifshitz, E. M. Pitaevskii, *Statistical Physics* (Butterworth-Heinemann, New York, 1999).
3. K. G. Wilson, J. Kogut, *Phys. Rep.* **12**, 75 (1974).
4. The Landau paradigm is also known to fail near 1D quantum critical points (or 2D classical critical points), such as the model considered by Haldane (25). This failure is caused by strong fluctuations in a low-dimensional system, a mechanism that does not generalize to higher dimensions.
5. R. B. Laughlin, *Adv. Phys.* **47**, 943 (1998).
6. C. Lannert, M. P. A. Fisher, T. Senthil, *Phys. Rev. B* **63**, 134510 (2001).
7. T. Senthil, L. Balents, S. Sachdev, A. Vishwanath, M. P. A. Fisher, <http://xxx.lanl.gov/abs/cond-mat/0312617>.
8. A. Vishwanath, L. Balents, T. Senthil, <http://xxx.lanl.gov/abs/cond-mat/0311085>.
9. D. S. Rokhsar, S. A. Kivelson, *Phys. Rev. Lett.* **61**, 2376 (1988).
10. R. Moessner, S. L. Sondhi, E. Fradkin, *Phys. Rev. B* **65**, 024504 (2002).
11. F. D. M. Haldane, *Phys. Rev. Lett.* **61**, 1029 (1988).
12. S. Chakravarty, B. I. Halperin, D. R. Nelson, *Phys. Rev. B* **39**, 2344 (1989). These authors correctly noted that the Berry phases could at least be neglected in the Néel phase, but perhaps not beyond it; their critical theory applies to square lattice models with the spin  $S$  an even integer (but not to  $S$  half-odd-integer) and to dimerized or double-layer antiferromagnets with an even number of  $S = 1/2$  spins per unit cell [such as the model in (13)].
13. M. Troyer, M. Imada, K. Ueda, *J. Phys. Soc. Jpn.* **66**, 2957 (1997).
14. N. Read, S. Sachdev, *Phys. Rev. Lett.* **62**, 1694 (1989).
15. A. V. Chubukov, S. Sachdev, J. Ye, *Phys. Rev. B* **49**, 11919 (1994). Speculations on the dangerous irrelevance of Berry phase effects appeared here.
16. Halperin *et al.* (26) studied the critical theory of  $L_z$  using expansions in  $4 - D$  ( $D$  is the dimension of spacetime) and in  $1/N$ . The former yielded a first-order transition and the latter second-order transition. Subsequent duality and numerical studies (17, 20) have shown the transition is second-order in  $D = 3$  for  $N = 1, 2$ .
17. O. Motrunich, A. Vishwanath, <http://xxx.lanl.gov/abs/cond-mat/0311222>.

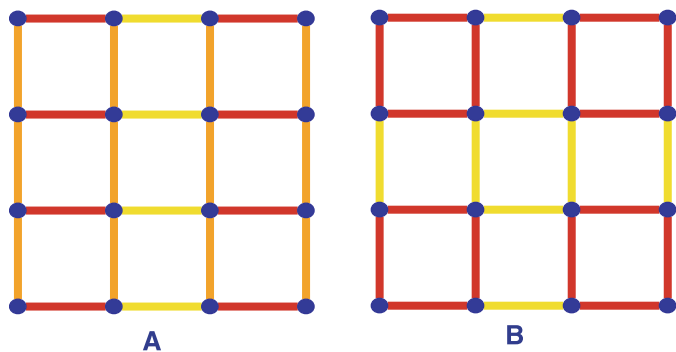


**Fig. 4.** Pattern of symmetry-breaking in the two possible VBS states (A and B) predicted by Eq. 8. The last term in Eq. 8 leads to a potential,  $-\lambda \cos[4(\theta_1 - \theta_2)]$ , and the sign of  $\lambda$  chooses between the two states above. The distinct lines represent distinct values of  $\langle \hat{S}_z \cdot \hat{S}_r \rangle$  on each link. Note that the state in (A) is identical to that in Fig. 1B.

18. Scaling analyses, generalizations, and physical consequences appear in the supporting material on *Science Online*.
19. S. Sachdev, K. Park, *Ann. Phys. N.Y.* **298**, 58 (2002).
20. C. Dasgupta, B. I. Halperin, *Phys. Rev. Lett.* **47**, 1556 (1981).
21. A. W. Sandvik, S. Daul, R. R. P. Singh, D. J. Scalapino, *Phys. Rev. Lett.* **89**, 247201 (2002).
22. C. Lhuillier, G. Misguich, <http://xxx.lanl.gov/abs/cond-mat/0109146>.
23. P. Coleman, C. Pépin, Q. Si, R. Ramazashvili, *J. Phys. Condens. Matt.* **13**, 723 (2001).
24. Q. Si, S. Rabello, K. Ingersent, J. L. Smith, *Nature* **413**, 804 (2001).
25. F. D. M. Haldane, *Phys. Rev. B* **25**, 4925 (1982).
26. B. I. Halperin, T. C. Lubensky, S.-k. Ma, *Phys. Rev. Lett.* **32**, 292 (1974).
27. This research was generously supported by NSF under grants DMR-0213282, DMR-0308945 (T.S.), DMR-9985255 (L.B.), DMR-0098226 (S.S.), and DMR-0210790 and PHY-9907949 (M.P.A.F.). We also acknowledge funding from the NEC Corporation (T.S.), the Packard Foundation (L.B.), the Alfred P. Sloan Foundation (T.S. and L.B.), a Pappa-

lardo Fellowship (A.V.), and an award from The Research Corporation (T.S.). We thank the Aspen Center for Physics for hospitality.

## Supporting Online Material

[www.sciencemag.org/cgi/content/full/303/5663/1490/DC1](http://www.sciencemag.org/cgi/content/full/303/5663/1490/DC1)

SOM Text

References and Notes

23 September 2003; accepted 7 January 2004

## REPORTS

## Terahertz Magnetic Response from Artificial Materials

T. J. Yen,<sup>1\*</sup> W. J. Padilla,<sup>2\*</sup> N. Fang,<sup>1\*</sup> D. C. Vier,<sup>2</sup> D. R. Smith,<sup>2</sup> J. B. Pendry,<sup>3</sup> D. N. Basov,<sup>2</sup> X. Zhang<sup>1†</sup>

We show that magnetic response at terahertz frequencies can be achieved in a planar structure composed of nonmagnetic conductive resonant elements. The effect is realized over a large bandwidth and can be tuned throughout the terahertz frequency regime by scaling the dimensions of the structure. We suggest that artificial magnetic structures, or hybrid structures that combine natural and artificial magnetic materials, can play a key role in terahertz devices.

The range of electromagnetic material response found in nature represents only a small subset of that which is theoretically possible. This limited range can be extended by the use of artificially structured materials, or metamaterials, that exhibit electromagnetic properties not available in naturally occurring materials. For example, artificial electric response has been introduced in metallic wire grids or cell meshes, with the spacing on the order of wavelength (*1*); a diversity of these meshes are now used in THz optical systems (*2*). More recently, metamaterials with subwavelength scattering elements have shown negative refraction at microwave frequencies (*3*), for which both the electric permittivity and the magnetic permeability are simultaneously negative. The negative-index metamaterial relied on an earlier theoretical prediction that an array of nonmagnetic conductive elements could exhibit a strong, resonant response to the magnetic component of an electromagnetic field (*4*). In the present work, we show that an inherently nonmagnetic metama-

terial can exhibit magnetic response at THz frequencies, thus increasing the possible range in which magnetic and negative-index materials can be realized by roughly two orders of magnitude.

Conventional materials that exhibit magnetic response are far less common in nature than materials that exhibit electric response, and they are particularly rare at THz and optical frequencies. The reason for this imbalance is fundamental in origin: Magnetic polarization in materials follows indirectly either from the flow of orbital currents or from unpaired electron spins. In magnetic systems, resonant phenomena, analogous to the phonons or collective modes that lead to an enhanced electric response at infrared or higher frequencies, tend to occur at far lower frequencies, resulting in relatively little magnetic material response at THz and higher frequencies.

Magnetic response of materials at THz and optical frequencies is particularly important for the implementation of devices such as compact cavities, adaptive lenses, tunable mirrors, isolators, and converters. A few natural magnetic materials that respond above microwave frequencies have been reported. For example, certain ferromagnetic and antiferromagnetic systems exhibit a magnetic response over a frequency range of several hundred gigahertz (*5–7*) and even higher (*8, 9*). However, the magnetic effects in these materials are typically weak and often exhibit narrow bands (*10*), which limits the scope of possible THz devices. The realization of magnetism at THz and higher

frequencies will substantially affect THz optics and their applications (*11*).

From a classical perspective, we can view a magnetic moment as being generated by microscopic currents that flow in a circular path. Such solenoidal currents can be induced, for example, by a time-varying magnetic field. Although this magnetic response is typically weak, the introduction of a resonance into the effective circuit about which the current flows can markedly enhance the response. Resonant solenoidal circuits have been proposed as the basis for artificially structured magnetic materials (*12*), although they are primarily envisaged for lower radio-frequency applications. With recent advances in metamaterials, it has become increasingly feasible to design and construct systems at microwave frequencies with desired magnetic and/or electric properties (*3, 13, 14*). In particular, metamaterials promise to extend magnetic phenomena because they can be designed to

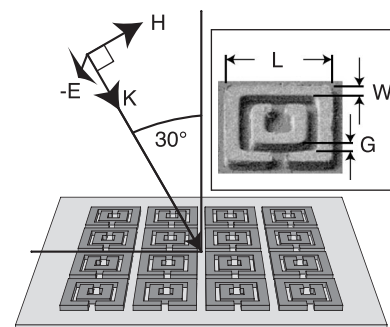


**Fig. 1.** Illustration depicting the orientation of the 30° ellipsometry experiment. The polarization shown is S-polarization, or transverse electric, for excitation of the magnetic response. P-polarization, transverse magnetic, was also measured. (Inset) A secondary ion-beam microscopy image of sample D1, taken by focused ion-beam microscopy. For each SRR, the split gap is 2 μm. The corresponding gap between the inner and outer ring (*G*), the width of the metal lines (*W*), the length of the outer ring (*L*), and the lattice parameter were 2, 4, 26, and 36 μm for sample D1; 3, 4, 32, and 44 μm for sample D2, and 3, 6, 36, and 50 μm for sample D3, respectively. These values were used in both design and simulation. *K*, the wave vector of incident light; *H*, the magnetic field intensity; *-E*, the electrical field intensity.

<sup>1</sup>Department of Mechanical and Aerospace Engineering, University of California at Los Angeles, 420 Westwood Plaza, Los Angeles, CA 90095, USA. <sup>2</sup>Department of Physics, University of California, San Diego, 9500 Gilman Drive, La Jolla, CA 92093-0319, USA. <sup>3</sup>Condensed Matter Theory Group, The Blackett Laboratory, Imperial College, London SW7 2AZ, UK.

\*These authors contributed equally to this work.

†To whom correspondence should be addressed. E-mail: [xiang@seas.ucla.edu](mailto:xiang@seas.ucla.edu)